MEDICAL SCIENCE MONITOR

ANIMAL STUDY

e-ISSN 1643-3750
© Med Sci Monit, 2017; 23: 3373-3382
DOI: 10.12659/MSM.902528

Received: 2016.11.25
Accepted: 2016.12.19
Published: 2017.07.12

In Vitro and *In Vivo* Investigation of High-Intensity Focused Ultrasound (HIFU) Hat-Type Ablation Mode

Authors' Contribution:
Study Design A
Data Collection B
Statistical Analysis C
Data Interpretation D
Manuscript Preparation E
Literature Search F
Funds Collection G

ABCDEFG Hongya Dai*
ABFG Fei Chen*
AF Sijing Yan
BD Xiaoya Ding
BC Dazhao Ma
BC Jing Wen
BD Die Xu
AG Jianzhong Zou

College of Biomedical Engineering, Chongqing Medical University, State Key Laboratory of Ultrasound Engineering in Medicine Co-Founded by Chongqing and The Ministry of Science and Technology, Key Laboratory of Ultrasound in Medicine and Engineering, Chongqing, P.R. China

* These authors contributed equally to this work

Corresponding Author: Jianzhong Zou, e-mail: 1109905304@qq.com

Source of support: This work was supported by the National Basic Research Program of China (No. 2011CB707900), the National Natural Science Fund of the Chinese National Science Foundation (No. 81127901, 11574039, and 11274404), the National Instrumentation Program (No. 2013YQ030629), and the Graduate Student Research Innovation Project of the Chongqing Municipal Education Commission (No. CYS14106)

Background: The aim of this study was to investigate the feasibility of the application of high-intensity focused ultrasound (HIFU) hat-type ablation mode in *in vitro* and *in vivo* models, and to compare the ablation effects of different parameter combinations.

Material/Methods: HIFU hat-type ablation was performed in isolated bovine liver tissue and in the liver tissue in living rabbits, and the coagulative necrosis for different parameter combinations (plane angles and irradiation order) was investigated. We also analyzed and compared the ablation effects of traditional ablation and hat-type ablation modes. Coagulative necrosis morphology was detected with TTC staining, and the coagulative necrosis volume and energy efficiency factor (EEF) were calculated and compared.

Results: Coagulative necrosis was observed in all the ablated groups, and the coagulative necrosis volume was much larger than the irradiation area. The coagulative necrosis induced by the hat-type ablation was more regular and controllable than the traditional ablation. The angles between the ablation planes determined the coagulative necrosis morphology, but did not affect the coagulative necrosis volume. Moreover, the irradiation order significantly influenced the coagulative necrosis. Importantly, under certain conditions, hat-type ablation achieved higher efficiency compared with the traditional ablation mode.

Conclusions: Compared with the traditional ablation mode, HIFU hat-type ablation effectively shortened the irradiation time, reduced the over-accumulation of energy, and increased the HIFU ablation efficiency.

MeSH Keywords: Ablation Techniques • High-Intensity Focused Ultrasound Ablation • *In Vitro*

Full-text PDF: http://www.medscimonit.com/abstract/index/idArt/902528

Indexed in: [Current Contents/Clinical Medicine] [SCI Expanded] [ISI Alerting System] [ISI Journals Master List] [Index Medicus/MEDLINE] [EMBASE/Excerpta Medica] [Chemical Abstracts/CAS] [Index Copernicus]

Background

High-intensity focused ultrasound (HIFU) is a type of micro- or non-invasive local physical therapy undergoing rapid development in the 21th century. It is widely used in the clinical treatment of various benign and malignant solid tumors [1–3]. However, only limited focal domains (within the range of millimeters) can be induced by the single exposure point in HIFU, and the ultrasonic energy decays in the propagating pathway in an exponential manner [4]. Moreover, the blood flow consumes some of the energy. Therefore, it takes the traditional point-line-plane-volume HIFU ablation mode hours to ablate a tumor, suggesting relatively low efficiency [5–7]. Insufficient treatment duration might result in tissue remnants, while extended treatment time is be associated with increased medical cost and clinical risk. Therefore, it is of great importance to develop a therapeutic HIFU mode that is safer, more efficient, and more convenient. In recent years, studies on improving the efficiency of HIFU ablation have focused on altering the acoustic environment to achieve HIFU enhancement, such as vascular embolization [8] and acoustic contrast agents [9,10], but these are limited by insecurity, material instability, and operational complexity.

During the propagation process, ultrasound can reflex, refract, and scatter, and higher tissue density is associated with stronger ultrasound reflection, and strong reflection occurs when ultrasound encounters gas. Coagulative necrosis formation changes the tissue characteristics and increases the tissue density, which, together with the thermal and mechanical effects of high-intensity ultrasound, leads to the formation of many vacuoles and water bubbles [11,12], resulting in extensive ultrasound reflection. Therefore, the present study is the first to show that the hat-type ablation mode, which is formed by 2 ablation planes with a certain angle between each other deep in the tumor tissue, is associated with enhanced ultrasound reflection and reduced ultrasound energy in the tissue behind and/or surrounding the target area. However, the energy decay of ultrasound during the propagation process is also accompanied by energy deposition. It has been already found that, under the same conditions, more energy of the *in vitro* irradiation is needed for deeper tissue [13]. It has also been clinically shown that when uterine fibroids are treated with HIFU, patients often report feeling burning in the treatment area, as well as groin discomfort, in addition to adverse effects such as skin irritation in the treatment area, gastrointestinal injury, and bladder injury [9,14], suggesting ultrasound energy deposition outside the focal spots and target areas. Therefore, in the present study we constructed a hat-shaped coagulative necrosis zone deep in the tumor tissue (the hat-type ablation mode), with no energy deposition within the hat structure, to accelerate the limited energy deposition within the hat structure to produce coagulative necrosis, improve energy utilization, and increase ablation efficiency.

In this study, HIFU hat-type ablation was performed using *in vitro* and *in vivo* experimental setups, which confirmed the feasibility of the hat-type ablation mode. Moreover, the optimal parameters were investigated via observing the coagulative necrosis sizes and morphological characteristics under different combinations of irradiation conditions. We also analyzed and compared the ablation features and effects between the traditional and hat-type ablation modes.

Material and Methods

HIFU hat-type ablation

The JC200 Focused Ultrasound Tumor Therapeutic System was provided by Chongqing HIFU Medical Technology Co., Ltd. (Chongqing, China). The system consisted of the following functional parts: the ultrasound transducer/treatment head, double concave spherical focus (with outer and inner diameters of 220 mm and 80 mm, respectively), with a real-time monitoring ultrasound probe integrated in the central opening location, with a frequency of 0.9 MHz and a focus distance of 160 mm; the treatment bed (the bed plate and the movement system); the image monitoring system, including the color Doppler ultrasound diagnostic apparatus (Esaote, Italy; with a probe frequency range of 3.5–5.0 MHz) and the GrayAnalyse image gray-scale analysis software; the computer terminal controlling system and related software; the power source and water treatment system; and Grayval HIFU measurement software (Chongqing HIFU Medical Technology Co., Ltd.).

For the hat-type ablation, the planes with a certain angle were ablated with ultrasound energy in the deepest target tissue. Briefly, the y and z axes were moved on the same level, to ablate tow lines with same length and a certain angle, and then the x axis was moved on different levels to repeat the above irradiation performance, to finally form 2 planes with a specific angle (Figure 1). Thereafter, the parameter combinations, including the angles and the irradiation orders, were changed to form the hat structure.

Isolated bovine liver tissue and grouping

Fresh bovine liver tissue within 6 h of slaughter was provided by the Jiangbei Slaughter House, Chongqing, China. The tissue was first cut into 80×80×60 mm cubes, which were washed and degassed in vacuum for 30–60 min, and then placed in the degassed water until use.

Indexed in: [Current Contents/Clinical Medicine] [SCI Expanded] [ISI Alerting System] [ISI Journals Master List] [Index Medicus/MEDLINE] [EMBASE/Excerpta Medica] [Chemical Abstracts/CAS] [Index Copernicus]

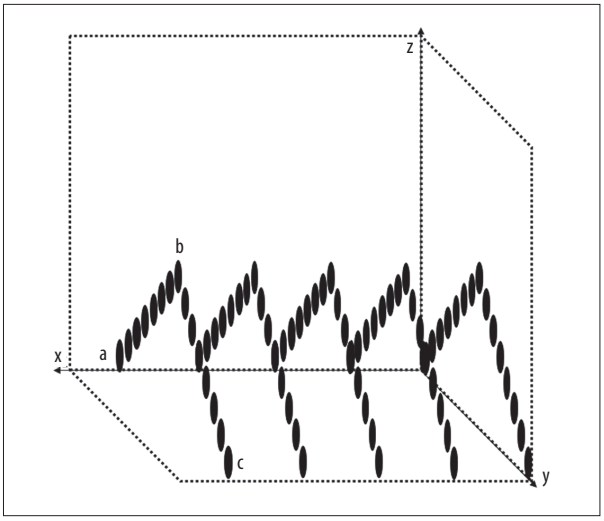

Figure 1. Schematic plot for hat-type ablation. A hat structure was formed by 2 planes with the certain angle.

The bovine liver tissue was divided into the following groups (10 pieces of bovine liver tissue each group): (1) Group A, in which the irradiation order was a→b→c, including Subgroup A1, A2, and A3; (2) Group B, in which the irradiation order was a→b→c, →b→a, with the angle of 90°; and (3) Group C (the control group), in which the traditional irradiation mode was applied. The detailed irradiation parameters and conditions are shown in Table 1.

HIFU hat-type ablation on *in vitro* bovine liver tissue

The fully degassed bovine liver tissue was mounted on the treatment bed, and the planes with fewer blood vessels and hepatic ducts were selected for HIFU treatment via moving the x, y, and z axes under ultrasound monitoring, with the continuous wave and point manner (setting the power at 250 W, and single-point irradiation time of 2 s).

For Subgroup A1, the y axis was moved towards the positive direction for 1 mm, and the z axis was moved towards the positive direction for 2 mm, with a total of 10 movements for both the y and z axes, with 10 irradiation points to form a line. Then the y axis was moved towards the same direction, once for 1 mm, and the z axis was moved towards the negative direction, once for 2 mm. A total of 9 movements formed another line, and the angles between these 2 lines was 55°. Thereafter, the x axis was moved 5 times, 5 mm once, to obtain 2 planes with the angle of 55°. For Subgroup A2, the y and z axes were moved 2 mm each time, and the HIFU irradiation was performed in the same manner, to form 2 planes with the angle of 90°. For Subgroup A3, the y axis was moved 2 mm, and the z axis was moved 1 mm, each time, to form 2 planes with the angle of 125°.

For group B, the same irradiation parameters as with Subgroup A2 were applied, except that the irradiation order was changed into a→b→c, →b→a, so that when the first irradiation plane was finished, the next plane was irradiated in the opposite order. The plane irradiation times were both 95 for groups A and B, both with a total of5 planes, and 19 points on each plane.

For group C (the control group), the isolated bovine liver tissue was ablated with the traditional point-line-plane-volume combination scanning mode. The depths for all planes were the same as with subgroup A2 (38, 36, 34,..., 22, and 20 mm), and the ablation was conducted point by point, with the ablation lengths on each plane equal to the distances between the 2 points on corresponding lines in subgroup A2. The coagulative necrosis degree was determined based on the gray-scale change in the focal point during the ablation, and the irradiation parameters were adjusted accordingly. The power range was set at over 200 W to 250 W, and the distance between the irradiation points was adjusted based on the gray-scale change (under the condition of a very strong signal, the irradiation focus would be moved to the edge of the strong-echo area to continue the ablation). The distances between planes were 5 mm, with a total of 5 ablation planes. The distance between the lowest irradiation point and the base plane was 20 mm for groups A, B, and C, with the ablation interval of

Table 1. Irradiation parameters for the isolated bovine liver tissue.

	Group A			Group B	Group C
	A1	A2	A3		
N	10	10	10	10	10
Single-point irradiation duration (s)	2	2	2	2	–
Irradiation power (W)	250	250	250	250	200–250
Line distance (mm)	5	5	5	5	5
Irradiation planes	5	5	5	5	5
Irradiation order	a→b→c	a→b→c	a→b→c	a→b→c, →b→a	–

Indexed in: [Current Contents/Clinical Medicine] [SCI Expanded] [ISI Alerting System] [ISI Journals Master List] [Index Medicus/MEDLINE] [EMBASE/Excerpta Medica] [Chemical Abstracts/CAS] [Index Copernicus]

3 min between the ablation planes. All the ablation procedures for these groups were completed 1 time. The total irradiation time and ablation energy were recorded for groups A, B, and C.

Experimental animals and grouping

A total of 50 healthy New Zealand white rabbits, male or female, weighing 2.0–2.5 kg, were provided by the Animal Center of Chongqing Medical University. All animal experimental procedures were approved by the Animal Ethics Committee of Chongqing Medical University. These rabbits were divided into the following groups (n=10): (1) group D, including 3 subgroups (subgroup D1, D2, and D3, with the plane angles of 55°, 90°, and 125°, respectively); (2) group E, in which the hat-type ablation was applied, with the irradiation angle of 90° and the irradiation order of a→b→c, →b→a; and (3) group F, the control group, in which traditional irradiation was performed.

HIFU hat-type ablation on *in vivo* liver tissue in rabbits

Before the irradiation treatment, the rabbits were fasted for 1–2 d. The abdominal fur was removed with 8% Na_2S, from 20–30 mm above the xiphoid to the hind leg root, covering an area of about 30–40 mm outside the nipples. The rabbits were anesthetized with 3% pentobarbital sodium, and fixed on the treatment bed in prone position. Healthy rabbit liver tissue was subjected to hat-type ablation under the ultrasound monitoring, with the output power of 250 W.

Nine irradiation points were selected on each plane. For group D (including the 3 subgroups), the irradiation mode was the same as for group A in the HIFU hat-type ablation on isolated bovine liver tissue, with 5 ablation planes. For group E, the ablation mode was the same as for group B in the HIFU hat-type ablation on isolated bovine liver tissue, with 4 ablation planes. During the irradiation, the single-point irradiation time was adjusted according to the gray-scale change in the target area. For group F, the same irradiation mode as for group C in the HIFU hat-type ablation on isolated bovine liver tissue was applied, with a total of 4 ablation planes. The lowest irradiation point was 20 mm from the skin, and the distance between the ablation planes was 3 mm. The single-point irradiation duration was 1–2 s. All the ablation procedures for these groups were completed at 1 time. The total irradiation time and ablation energy were recorded.

Coagulative necrosis volume measurement

For the coagulative necrosis volume measurement in the *in vitro* model, the cooling bovine liver was cut into 3–5-mm slices along the ultrasound long axis. The tissue sections were immersed in 1% triclosan tetrazolium chloride and kept at 37°C for 20 min. After washing with PBS, the coagulative necrosis morphology was observed, and the coagulative necrosis volume was measured. For the observation of the coagulative necrosis morphology, the aspect ratio was calculated as the ratio between the long axis along the acoustic beam direction and the short axis perpendicular to the acoustic beam direction. To obtain the coagulative necrosis volume, necrotic tissue was converted into regular shape with the cut-and-fill method, and the length, width, and thickness of the necrotic tissue were measured to calculate the volume according to the following formulation: Volume=length × width × thickness. We then calculated the energy efficiency factor (EEF) with the following formulation: $EEF=\eta \cdot P \cdot t/V$, in which η was the focusing coefficient of the HIFU transducer, P (W) was the sound power, t (s) was the irradiation time, and V (mm^3) was the coagulative necrosis volume.

For the *in vivo* model, the rabbits were sacrificed 2–3 d after irradiation, and the intact liver was removed. The coagulative necrosis morphology was observed, and the coagulative necrosis volume was measured as described above.

Histological observation

For the *in vitro* and the *in vivo* irradiation, the tissue from the following regions were subjected to HE staining and observation under a light microscope: in the hat-type ablation groups, tissue beneath the hat structure, as well as at the junction of the irradiated area and the surrounding normal tissue; and in the traditional ablation groups, tissue in the irradiation area and at the junction area.

Statistical analysis

Data are expressed as mean ±SD. SPSS 20.0 software was used for statistical analysis. Analysis of variance was performed for the comparison of coagulative necrosis morphology and volume between groups, and *t* test was used for the comparison of group means. $p<0.05$ was considered statistically significant.

Results

Coagulative necrosis of *in vitro* bovine liver tissues after ablation

The coagulative necrosis of the irradiated bovine liver tissue was first investigated. Our results showed obvious coagulative necrosis in all groups (A, B, and C). In groups A and B, the coagulative necrosis was spread out from the irradiation focus to the area beneath the hat structure, and the necrotic volume was much larger than the irradiation area, especially for group B. Coagulation necrotic tissue was gray in color, and exhibited triangular morphology. TTC staining showed white

Indexed in: [Current Contents/Clinical Medicine] [SCI Expanded] [ISI Alerting System] [ISI Journals Master List] [Index Medicus/MEDLINE] [EMBASE/Excerpta Medica] [Chemical Abstracts/CAS] [Index Copernicus]

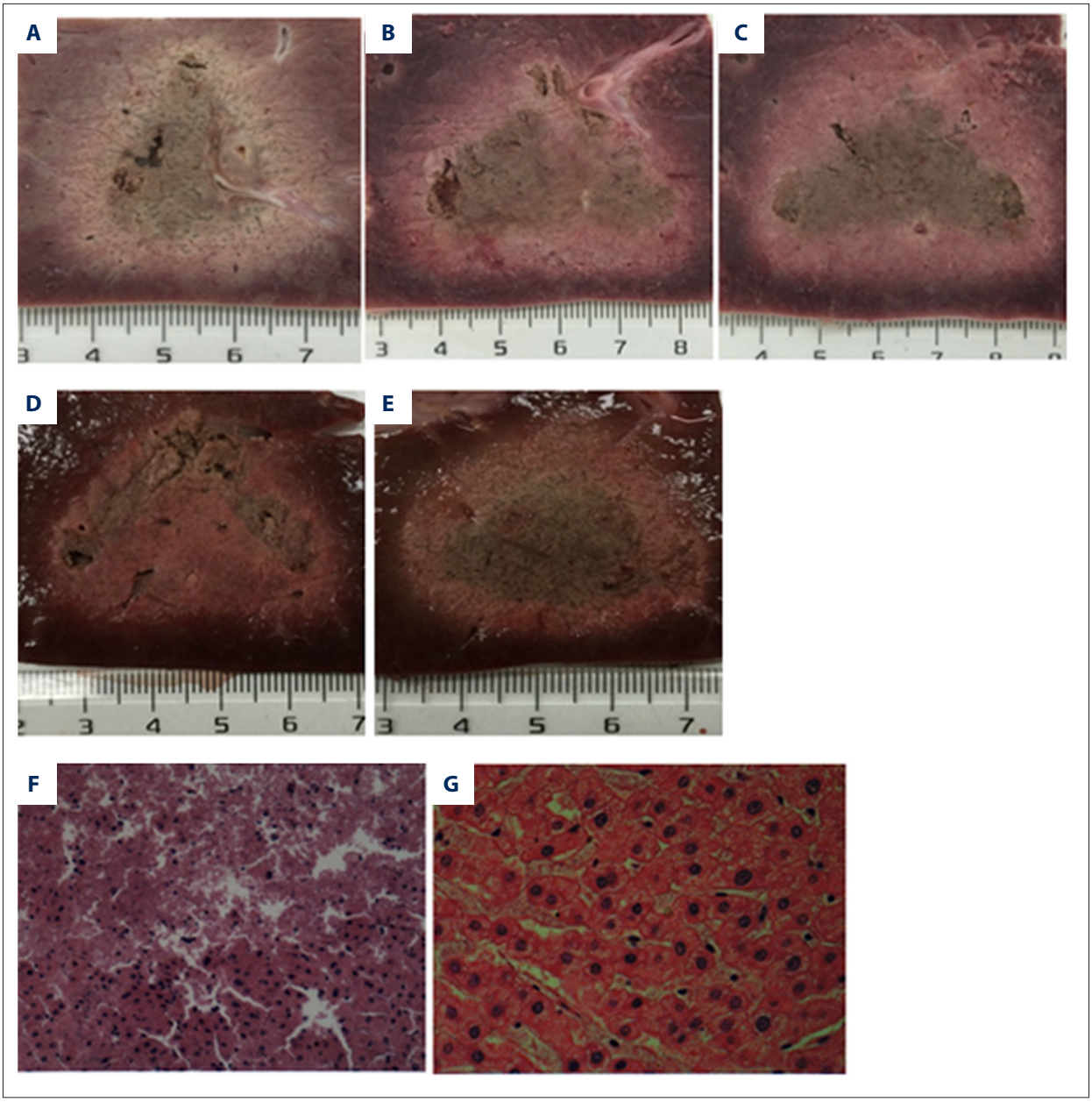

Figure 2. Gross and histological observation of *in vitro* bovine liver tissues after ablation. (**A–C**) The ablation with the plane angles of 55° (**A**), 90° (**B**), and 125° (**C**), respectively. (**D**) The experimental group, with the irradiation order of a→b→c, →b→a. (**E**) The control group, in which the traditional ablation mode was applied. HE staining was performed for histological observation. (**F**) A clear boundary was observed between the irradiation region and surrounding tissue in the *in vitro* bovine liver (×200). (**G**) In the tissue under the hat structure, cytoplasm was lightly stained, nuclear condensation was observed, and the hepatic plate structure had disappeared (× 400).

necrotic tissue, and the normal bovine liver tissue was pink. Moreover, in groups A and B, clear boundaries were observed between the coagulated necrotic tissue and the normal tissue behind the hat structure. In group C, coagulative necrosis was noted over the whole irradiated area, with a visible boundary between the irradiated and peripheral normal tissues (Figure 2A–2E).

After slicing, some of the coagulated necrotic liver tissue was pulverized. Under light microscopy, the cell structure in the irradiated area had disappeared, and the nuclei were condensed, fragmented, and/or dissolved, or associated with mesh-like structure (Figure 2F). In the non-irradiated area beneath the hat structure, the hepatic plate structure had disappeared, and obvious swollen cells were observed, with

Indexed in: [Current Contents/Clinical Medicine] [SCI Expanded] [ISI Alerting System] [ISI Journals Master List] [Index Medicus/MEDLINE] [EMBASE/Excerpta Medica] [Chemical Abstracts/CAS] [Index Copernicus]

Table 2. Ablation effects in isolated bovine liver tissue.

	Group A			Group B	Group C
	A1	A2	A3		
Ablation duration (s)	190±0.00	190±0.00	190±0.00	190±0.00	389.80±3.70
Energy consumption (J)	47500±0.00	47500±0.00	47500±0.00	47500±0.00	78160.80±1024.79
Coagulated necrosis volume (mm^3)	19305.09±1132.65	19213.13±228.09	18998.13±991.01	29484.89±1553.53	31164.39±1622.67
EEF (J/mm^3)	1.66±0.10	1.66±0.04	1.68±0.09	1.13±0.06#	1.76±0.07
Aspect ratio	1.50±0.005#	0.77±0.007#	0.59±0.011#	1.25±0.016	0.86±0.019

Compared with the other two groups, $P<0.05$.

lightly stained cytoplasm, pyknotic nuclei, and no continuity (Figure 2G).

On the other hand, as shown in Table 2, our results from the coagulative necrosis volume measurement showed no significant differences in EEF between the subgroups in group A and group C ($p>0.05$), while the total irradiation time in group A was obviously shorter than in group C. Moreover, in group B, all the irradiation time, energy, and EEF values were significantly less than in group C ($p<0.05$); while between groups A and B, only significantly different EEF values were observed ($p<0.05$). Furthermore, no significant differences were observed between subgroups A1, A2, and A3 ($p>0.05$). In these subgroups, the aspect ratios were decreased with increasing angles ($p<0.01$), while no significant differences were observed in necrotic volume ($p>0.05$).

Coagulative necrosis of *in vivo* rabbit liver tissue after ablation

The coagulative necrosis in the rabbit liver tissue with different irradiation angles was investigated. Our results showed that, in subgroups D1, D2, and D3, coagulation necrotic tissue larger than the irradiation area was observed, with gray color and a clear boundary between the irradiated necrotic and surrounding normal tissues. In subgroup D1, the necrotic volume was 3907.85±565.53 mm^3, with the aspect ratio of 2.14±0.25 (Figure 3A); in subgroup D2, the necrotic volume was 4431.49±721.36 mm^3, with the aspect ratio of 1.47±0.26 (Figure 3B); and in subgroup D3, the coagulated necrotic volume was 3729.46±1049.29 mm^3, with the aspect ratio of 1.06±0.12 (Figure 3C). Similar to the *in vitro* results, the increasing angles between the planes lead to decreasing aspect ratios of the coagulated necrotic tissue ($p<0.01$), without significantly increased coagulated necrosis volumes.

For the experimental groups, coagulative necrosis was observed in each rabbit, and the necrotic tissue was spread towards the inside of the hat structure. The necrotic volume was much larger than the irradiation area, and sharp boundaries were observed between the necrotic and normal tissues (Figure 3D). No significant adverse reactions were observed in any rabbits. For the control group, coagulative necrosis was observed in each rabbit, with irregular necrotic morphology, and the boundary between the necrotic and normal tissue was visible (Figure 3E). For the histological observation, cell structure disappearance was observed in the irradiated area and the non-irradiated area beneath the hat structure in the experimental groups (Figure 3F), as well as in the coagulated necrosis areas in the control group. Clear, sharp boundaries were also observed between the necrotic and surrounding normal tissues in the experimental groups (Figure 3G). One of the rabbits in the control group suffered from gastric perforation after irradiation (Figure 4A), and died immediately, while another rabbit had a skin burn (Figure 4B). As shown in Table 3, the coagulative necrosis volume was 5087.55±806.85 mm^3 and the EEF value was 2.52±0.40 J/mm^3 in the experimental groups, while the coagulative necrosis volume was 5781.11±544.57 mm^3, and the EEF value was 3.11±0.39 J/mm^3 in the control group. No significant differences were observed in the necrotic volume between these 2 groups, and the EEF value in the experimental groups was smaller than in the control groups ($p<0.01$).

Discussion

High-intensity focused ultrasound (HIFU) is a non-invasive thermal ablation treatment method, which focuses the ultrasound on the *in vivo* tumor tissue and causes tissue necrosis via the thermal, cavitating, and mechanical effects. Due to the relatively satisfactory treatment outcomes, the clinical application of HIFU has been attracting more and more attention in recent years [15,16]. However, the application of HIFU in clinical settings has been limited by the low efficiency and unsatisfactory safety.

Indexed in: [Current Contents/Clinical Medicine] [SCI Expanded] [ISI Alerting System] [ISI Journals Master List] [Index Medicus/MEDLINE] [EMBASE/Excerpta Medica] [Chemical Abstracts/CAS] [Index Copernicus]

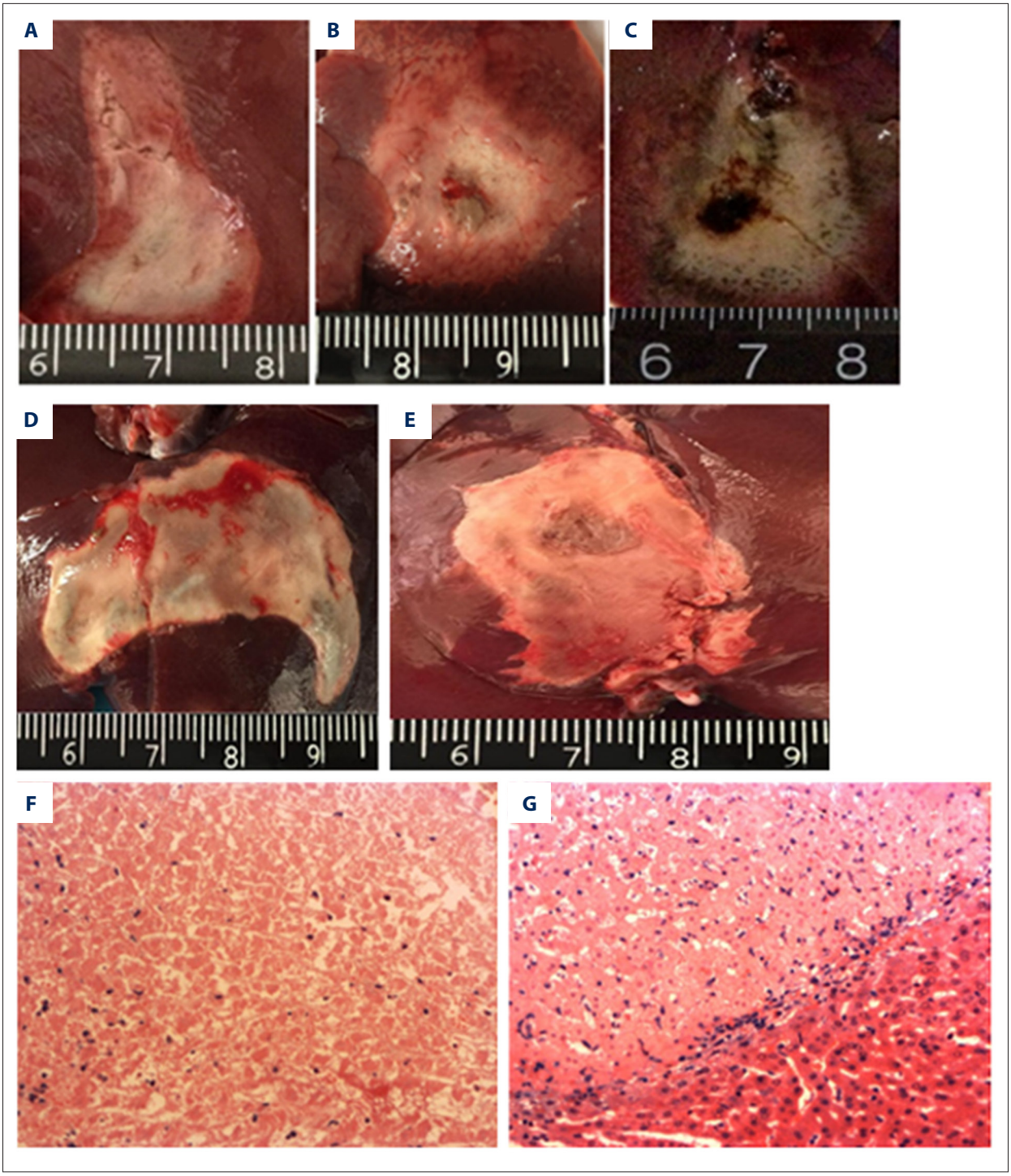

Figure 3. Rabbit liver sections with coagulative necrosis after ablation and its histological observation. (**A–C**) *In vivo* rabbit liver tissue was subjected to the hat-type ablation with the plane angles of 55° (**A**), 90° (**B**), and 125° (**C**), respectively. The tissue was sliced, and coagulative necrosis was observed. (**D**) The experimental group, with the irradiation order of a→b→c, →b→a. (**E**) The control group, in which the traditional ablation mode was applied. HE staining was performed for histological observation. (**F**) Obvious coagulative necrosis was noted beneath the hat structure, without any energy given, in the *in vivo* rabbit liver (×200). (**G**) A clearly, sharp boundary was observed between the coagulated necrotic region and the surrounding normal tissue in the *in vivo* rabbit liver (×200).

Indexed in: [Current Contents/Clinical Medicine] [SCI Expanded] [ISI Alerting System] [ISI Journals Master List] [Index Medicus/MEDLINE] [EMBASE/Excerpta Medica] [Chemical Abstracts/CAS] [Index Copernicus]

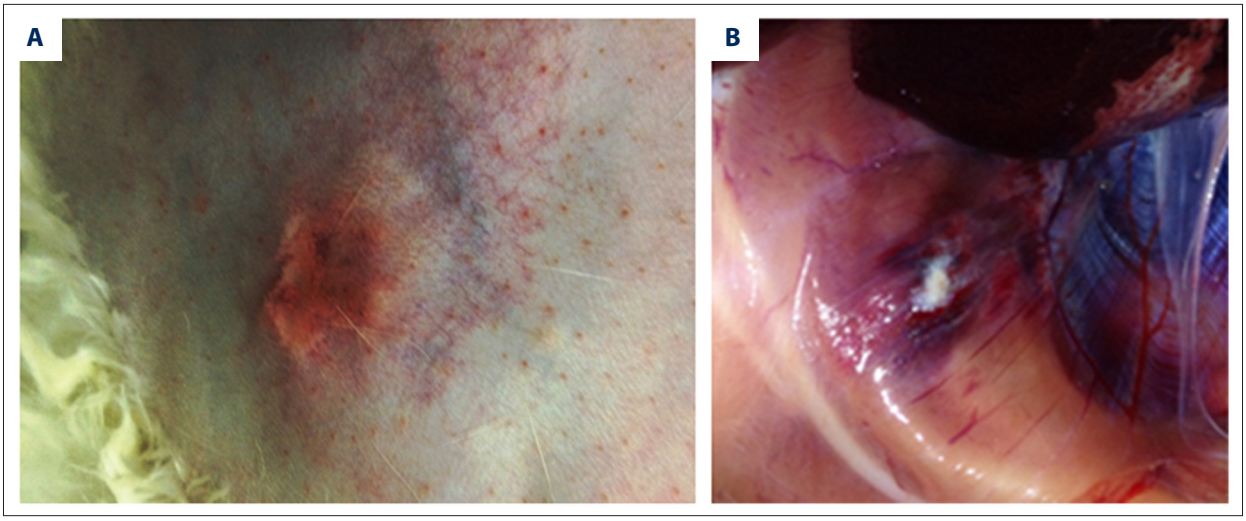

Figure 4. Complications in rabbits subjected to traditional irradiation. (**A**) Skin burn. (**B**) Gastric injury.

Table 3. Comparison of ablation effects between different ablation modes.

	Group E	Group F
Energy consumption (J)	17925.00±168.74	25450.00±998.61
Coagulated necrosis volume (mm^3)	5087.55±806.85	5781.11±544.57
EEF (J/mm^3)	2.52±0.40	3.11±0.39

HIFU treatment has been intensively investigated in various animal models and in humans. Zhou et al. [17] analyzed and compared the traditional irradiation mode *vs.* 2 spiral irradiation modes (from inside to outside and from outside to inside) in a gel model and *in vitro* bovine liver tissue. They showed that the novel irradiation modes can induce more even necrosis, and the optimized scanning path and dynamic parameters cause more even and intact injuries, leading to increased safety and efficiency of HIFU. Moreover, Bu et al. [5] have proposed the peripheral three-dimensional surface ablation mode, based on the fact that the edge of malignant tumor is characterized by excessive growth and is rich in blood supply, while the tissue inside the tumor is prone to undergo necrosis due to insufficient perfusion, as well as ischemia and hypoxia. This mode induces an intact coagulative necrosis region surrounding the tumor tissue, instead of irradiating the inside tissue. In the isolated bovine liver tissue and perfused pig liver models, the peripheral three-dimensional surface ablation mode is associated with significantly shorter irradiation time and reduced irradiation energy. In the present study, the hat-type ablation mode was established and applied in the *in vitro* and *in vivo* models. The coagulative necrosis was investigated under different conditions, in comparison with the control group, and the characteristics of the hat-type ablation and traditional irradiation were featured.

Our results show that, in the *in vitro* and *in vivo* models, coagulative necrosis was observed in all groups, and the necrotic volume was significantly larger than the irradiation area. The ultrasound energy could spread to the areas beneath the hat structure. This phenomenon could be explained as follows. Firstly, when the target tissue suffered from coagulative necrosis, the necrotic area was enlarged and the temperature was elevated in the surrounding tissues. The thermal effects would induce the diffusion of energy from the focal region (high temperature) to the non-irradiated region (low temperature) [17]. Secondly, because the acoustic attenuation coefficient and acoustic absorption coefficient in the coagulated tissues were increased compared with the surrounding tissues [18], together with that great number of micro-bubbles produced in the irradiated areas based on the cavitating effects, when the ultrasound reached the interface of coagulative necrotic tissues, significant scatter occurs, which prevents the sound waves from spread to the area behind the coagulative necrosis area, where the energy is accumulated in the near sound field surrounding the non-irradiated area [19]. Thirdly, during the process of irradiation, the ultrasound beam goes through the shallow surface of the target tissue, while the tissue in the near field absorbs the ultrasound energy [20]. When the energy was extensively accumulated, different injuries or even coagulative necrosis occur in the sound beam pathway. It has been shown that the temperature in the near field surrounding the HIFU focal region is elevated when subjected to ultrasound irradiation [20]. Moreover, other researchers have reported that, in the isolated muscle tissues treated with HIFU, when the temperature was dynamically recorded by the MRI temperature monitoring sequences (including the near and far fields of the focal region), the tissue temperature is increased

Indexed in: [Current Contents/Clinical Medicine] [SCI Expanded] [ISI Alerting System] [ISI Journals Master List] [Index Medicus/MEDLINE] [EMBASE/Excerpta Medica] [Chemical Abstracts/CAS] [Index Copernicus]

along with the increased HIFU irradiation duration and accumulated energy, and the temperature elevation expands towards the near field of the focal region as a conical surface, while the temperature in the far field of the focal region slowly rises and then gradually falls.

At present, HIFU treatment is mainly performed in China using ultrasound monitoring, while the coagulative necrosis in the target tissue is evidenced through gray-scale changes in the ultrasound image [21]. However, no obvious enhanced gray-scale signal is observed in the coagulative necrosis in the surrounding tissues with threshold temperature. Moreover, when the target tissues are mainly suffering from thermal effects with low dosage, the few micro-bubbles induced by the cavitating effects rapidly dissipate, leading to no obvious gray-scale changes in the sonogram. In the *in vivo* experiment, significant gray-scale changes were observed in some parts of the liver tissue, while no significant changes were noted in the other parts, indicating that only sufficient energy results in overall gray-scale changes. These phenomena can mislead clinicians to think that the target tissues did not receive enough energy, therefore leading to excessive energy accumulation and prolonged therapeutic duration, lowering the ablation efficiency. Our results showed that, in group C, part of the bovine liver tissue was powdery due to coagulative necrosis, suggesting excessive energy accumulation. It is well-accepted that prolonged treatment duration can lead to increased adverse reactions. A previous study has shown that, during the therapy, large amounts of ultrasound energy are accumulated in the body, overwhelming the body's regulation mechanisms, and resulting in increased body temperature as high as 39.2°C [22]. Long-term HIFU treatment can accidently cause adverse reactions. Our results showed that, in the hat-type ablation, no significant differences were observed in the EEF values between groups A and C, and the total irradiation time was significantly shorter than in the traditional irradiation groups. However, the irradiation time, energy, and EEF values in group B were all less than in group C, which is in line with the results of *in vivo* experiments, indicating that the hat-type ablation is superior to traditional irradiation mode, with increased ablation efficiency and decreased adverse reaction rate.

In the *in vitro* experiments, the coagulative necrosis was investigated with varying irradiating angles, irradiation orders, and conditions. Our results showed that, with the irradiation order of a→b→c, →b→a, the coagulative necrosis volume was significantly larger than with the irradiation order of a→b→c in group A. Because the energy produced in the focal point spreads out towards the surrounding tissues during HIFU irradiation, a region with a temperature of 42°C to 60°C would be expected (42°C is considered as the safe maximum temperature for normal tissues) [17]. The injuries induced by the energy can be reversed accumulated through multiple points, finally achieving the threshold temperature to induce irreversible necrosis. In group B, when the irradiation on one plane was finished, the energy was superimposed on the nearing point on the second plane to reduce energy waste. Accordingly, the control experiment was set up, and our results showed that the hat-type ablation mode significantly enhanced the HIFU irradiation compared with the traditional mode. In addition, changing the angle between the irradiation planes results in regular alterations in the coagulative necrosis morphology. In the *in vivo* experiments, irregular necrotic morphology is caused by the blood supply, postural changes, and respiratory dynamics, with the overall tear-drop ellipsoid-sphere shape. These results suggest that the energy outside the ablation area can be manipulated. Therefore, at the angle range of 125–180°, the morphology is changed towards the sphere-ellipsoid straight-line shape. However, no effects of angle changes on the coagulative necrosis volume were observed, which might be due to the limited sample size and measurement error. In the hat-type ablation group, the boundary between the coagulative necrotic tissue and the tissue behind the hat structure was clearly visible, with an overall triangular shape, while no regular boundary line was observed between the coagulative necrotic tissue and surrounding tissue in the traditional ablation group. These results suggest that the energy spread is controllable in the hat-type ablation, while the energy might be prone to spread towards the surrounding tissues in the traditional ablation mode. We speculate that when the tumor and surrounding tissues were adjacent to vital organs, the hat-type may be able to reduce the incidence of related adverse effects. In the control group, 1 rabbit had gastric perforation, and another had a skin burn, while no adverse reactions occurred in the experimental groups, with more regular overall necrotic morphologies. However, further in-depth studies are still needed to address this issue. Our results from the histological observation in the *in vitro* experiments showed that, in the ablated area, coagulative necrotic tissue was obvious, indicating that it was simple and feasible to completely ablate a hat-type structure in the tissue. In the *in vitro* experiments, beneath the hat structure, lightly stained cytoplasm and shrunken nuclei were observed, without nuclear fragmentation or dissolution. In the *in vivo* experiments, complete necrosis was observed in the irradiated region and in the non-irradiated area beneath the hat structure, possibly because, when the ablated region in the *in vitro* experiment was extended, the energy accumulated under the hat structure was not sufficient to induce complete necrosis, only leading to the necrotic status. In contrast, in the *in vivo* experiments the ablation area was limited and the accumulated energy was sufficient to cause complete necrosis beneath the hat structure. Rabbits were sacrificed at 2–3 d after irradiation, and the complete hat-type coagulative necrosis structure blocks the blood supply below, further leading to ischemia and hypoxia. Therefore, compared with the *in vitro* model, the coagulative necrosis was more complete and the morphology was more regular in the *in vivo* models.

Indexed in: [Current Contents/Clinical Medicine] [SCI Expanded] [ISI Alerting System] [ISI Journals Master List] [Index Medicus/MEDLINE] [EMBASE/Excerpta Medica] [Chemical Abstracts/CAS] [Index Copernicus]

Conclusions

We propose a novel ablation mode for FIHU: hat-type ablation. Under certain conditions, hat-type ablation can effectively shorten the irradiation time, reduced the over-accumulation of energy, and increase the HIFU ablation efficiency, providing an alternative clinical treatment option. However, our findings only demonstrate the feasibility of the HIFU hat-type ablation in ablating healthy liver tissue. Further in-depth studies are needed to investigate the application of the novel ablation mode in the clinical treatment of tumors.

Disclosures

All authors declare no financial and non-financial competing interests.

References:

1. Hwang JH, Crum LA: Current status of clinical high-intensity focused ultrasound. Conf Proc IEEE Eng Med Biol Soc, 2009; 2009: 130–33
2. Wu F, Wang ZB, Chen WZ et al: Extracorporeal focused ultrasound surgery for treatment of human solid carcinomas: Early Chinese clinical experience. Ultrasound Med Biol, 2004; 30: 245–60
3. Marinova M, Rauch M, Schild HH, Strunk HM: Novel non-invasive treatment with high-intensity focused ultrasound (HIFU). Ultraschall Med, 2016; 37: 46–55
4. Wang Z, Bai J, Li F et al: Microbubbles assist goat liver ablation by high intensity focused ultrasound. Eur Radiol, 2006; 16: 1557–63
5. Bu R, Yin L, Yang H et al: Tissue ablation accelerated by peripheral scanning mode with high-intensity focused ultrasound: A study on isolated porcine liver perfusion. Ultrasound Med Biol, 2013; 39: 1410–19
6. Kennedy JE: High-intensity focused ultrasound in the treatment of solid tumours. Nat Rev Cancer, 2005; 5: 321–27
7. Yu T, Fu X: Extracorporeal ultrasound-guided high intensity focused ultrasound: Implications from the present clinical trials. ScientificWorldJournal, 2014; 2014: 537260
8. Wu F, Wang ZB, Chen WZ et al: Advanced hepatocellular carcinoma: Treatment with high-intensity focused ultrasound ablation combined with transcatheter arterial embolization. Radiology, 2005; 235: 659–67
9. Peng S, Xiong Y, Li K et al: Clinical utility of a microbubble-enhancing contrast ("SonoVue") in treatment of uterine fibroids with high intensity focused ultrasound: A retrospective study. Eur J Radiol, 2012; 81: 3832–38
10. You Y, Wang Z, Ran H et al: Nanoparticle-enhanced synergistic HIFU ablation and transarterial chemoembolization for efficient cancer therapy. Nanoscale, 2016; 8: 4324–39
11. Haar GT, Rivens I, Chen L, Ridder S: High intensity focused ultrasound for treatment of rat tumor. Phys Med Biol, 1991; 36: 1495–501
12. Vaezy S, Shi X, Martin RW et al: Real-time visualization of high-intensity focused ultrasound treatment using ultrasound imaging. Ultrasound Med Biol, 2001; 27: 33–42
13. Ter HG, Sinnett D, Rivens I: High intensity focused ultrasound-a surgical technique for the treatment of discrete liver tumours. Phys Med Biol, 1989; 34: 1743–50
14. Cheng CQ, Zhang RT, Xiong Y et al: Contrast-enhanced ultrasound for evaluation of high-intensity focused ultrasound treatment of benign uterine diseases: Retrospective analysis of contrast safety. Medicine, 2015; 94: e729
15. Illing RO, Kennedy JE, Wu F et al: The safety and feasibility of extracorporeal high-intensity focused ultrasound (HIFU) for the treatment of liver and kidney tumours in a Western population. Br J Cancer, 2005; 93: 890–95
16. Al-Bataineh O, Jenne J, Huber P: Clinical and future applications of high intensity focused ultrasound in cancer. Cancer Treat Rev, 2012; 38: 346–53
17. Zhou Y, Kargl SG, Hwang JH: The effect of the scanning pathway in high-intensity focused ultrasound therapy on lesion production. Ultrasound Med Biol, 2011; 37: 1457–68
18. Bush NL, Rivens I, ter Haar GR, Bamber JC: Acoustic properties of lesions generated with an ultrasound therapy system. Ultrasound Med Biol, 1993; 19: 789–801
19. Sokka SD, King RK: MRI-guided gas bubble enhanced ultrasound heating in *in vivo* rabbit thigh. Phys Med Biol, 2003; 48: 223–41
20. Damianou C, Hynynen K: Focal spacing and near-field heating during pulsed high temperature ultrasound therapy. Ultrasound Med Biol, 1993; 19: 777–87
21. Fukuda H, Numata K, Nozaki A et al: Hyperecho in ultrasound images during high-intensity focused ultrasound ablation for hepatocellular carcinomas. Eur J Radiol, 2011; 80: 571–75
22. Yu T, Luo J: Adverse events of extracorporeal ultrasound-guided high intensity focused ultrasound therapy. PloS One, 2011; 6: 2053–56

Indexed in: [Current Contents/Clinical Medicine] [SCI Expanded] [ISI Alerting System] [ISI Journals Master List] [Index Medicus/MEDLINE] [EMBASE/Excerpta Medica] [Chemical Abstracts/CAS] [Index Copernicus]